RESEARCH PAPER

PCCP
www.rsc.org/pccp

Long-lived light-induced metastable states in *trans*-$[Ru(NH_3)_4(H_2O)NO]Cl_3 \cdot H_2O$ and related compounds

Dominik Schaniel,*[a] Theo Woike,[a] Bernard Delley,[b] Colette Boskovic,[c] Daniel Biner,[c] Karl W. Krämer[c] and Hans-Ueli Güdel[c]

[a] *Institut für Mineralogie & Geochemie, Universität zu Köln, Zülpicherstrasse 49b, 50674 Köln, Germany. E-mail: dominik.schaniel@uni-koeln.de*
[b] *Condensed Matter Theory, Paul Scherrer Institute, 5232 Villigen PSI, Switzerland*
[c] *Department of Chemistry and Biochemistry, University of Bern, Freiestr. 3, 3000 Bern 9, Switzerland*

Received 5th October 2004, Accepted 19th January 2005
First published as an Advance Article on the web 3rd February 2005

The existence of two light-induced long-lived metastable states SI, SII in irradiated *trans*-$[Ru(NH_3)_4(H_2O)NO]Cl_3 \cdot H_2O$ and *trans*-$[Ru(NH_3)_4(OH)NO]Cl_2$ is revealed by differential scanning calorimetry measurements and calculations based on density functional theory. Irradiation with light in the blue spectral range leads to the population of SI, while SII can be obtained by transferring SI into SII with irradiation of light in the near infrared spectral range. The population and transfer of the metastable states is described by exponential functions and the thermal decays are evaluated according to Arrhenius' law, yielding activation energies of $E_A(SI) = 0.95(3)$ eV, $E_A(SII) = 0.69(3)$ eV and frequency factors of $Z(SI) = 2 \times 10^{14}$ s^{-1}, $Z(SII) = 3 \times 10^{13}$ s^{-1} for *trans*-$[Ru(NH_3)_4(H_2O)NO]Cl_3 \cdot H_2O$, while $E_A(SI) = 0.91(3)$ eV, $E_A(SII) = 0.60(3)$ eV, $Z(SI) = 6 \times 10^{14}$ s^{-1}, $Z(SII) = 1 \times 10^{13}$ s^{-1} for *trans*-$[Ru(NH_3)_4(OH)NO]Cl_2$. The observations are compared with the ground state potential surface calculated by density functional theory, where the metastable states correspond to a *side-on* bonded (SII) and *isonitrosyl* (SI) configuration of the NO ligand. The calculations provide the energetic minima of the ground state and the metastable states SI and SII as well as the saddle points along the reaction coordinate Q, which corresponds roughly to a rotation of the NO ligand by about 90° (SII) and 180° (SI), and therefore allows for the comparison between observed and calculated activation energies.

I. Introduction

Ruthenium amine nitrosyl complexes are of significant interest due to their potential role as NO-carriers in biomedical applications.[1,2] Although some of the compounds of the form *trans*-$[Ru(NH_3)_4(L)NO]$ were already synthesized and described at the end of the 19th century[3] and further progress, including theoretical descriptions, have been reported since the middle of the 20th century, see *e.g.* refs. 4–9 and references therein, their remarkable properties in this respect were only detected recently.[10,11] Another equally exciting property of these nitrosyl-containing materials is their photosensitive behavior, which allows for the generation of long-lived metastable states upon illumination with visible light (generally in the blue spectral range). These light-induced metastable states are of relevance for technical applications, *e.g.*, holographic data storage.[12,13] Their major drawback is the fact that they are stable only at low temperatures, rendering them unsuitable for long-time storage or medical applications. However, since the 1977 discovery by Hauser *et al.*[14] of one metastable state in $Na_2[Fe(CN)_5NO] \cdot 2H_2O$ (SNP), a great deal of effort has been directed towards the synthesis of substances with metastable states that are stable above room temperature.[15–17] The lifetime at 300 K of the so-called metastable state SI could be increased from 1.1×10^{-4} s in SNP[18] to 1.8 s in $[Ru(NH_3)_5NO]Cl_3 \cdot H_2O$,[19] indicating that longer lifetimes can be obtained by variation of the ligands in these ruthenium compounds.

Here we report experimental and theoretical evidence for two metastable states SI and SII in *trans*-$[Ru(NH_3)_4(H_2O)NO]Cl_3 \cdot H_2O$ and *trans*-$[Ru(NH_3)_4(OH)NO]Cl_2$ using differential scanning calorimetry (DSC) and density functional theory (DFT). The activation energies E_A and frequency factors Z are determined from dynamic DSC measurements. They are compared with those determined for $[Ru(NH_3)_5NO]Cl_3 \cdot H_2O$[19] and with the calculated values for all these compounds. The population of SI and the transfer SI → SII are described as a function of irradiation wavelength and flux, as well as a function of temperature. An explanation of the observations is given by the calculation of the energetic minima and saddle points in the ground state potential surface, where the energetic minima correspond to a rotation of the NO ligand by about 90° (SII) and 180° (SI). In the following we will use this geometrical model for the description of the metastable states, since this model yields stable energetic minima in the DFT calculations and allows for the comparison of observed and calculated activation energies E_A. We have to mention that this geometrical model was confirmed up to now by X-ray diffraction for both metastable states,[20] while neutron diffraction experiments could not confirm the isonitrosyl configuration for SI in SNP.[21]

II. Experimental and computational details

Orange needle-shaped crystals of $[Ru(NH_3)_5NO]Cl_3 \cdot H_2O$ were prepared from $[Ru(NH_3)_5Cl]Cl_2$ (Strem Chemicals, 98%) according to a synthetic route previously described.[4] The well crystallized material was characterized by powder X-ray diffraction on a STOE diffractometer with Cu $K_{\alpha 1}$ radiation using a 0.3 mm capillary in transmission geometry. Peak positions and intensities are in very good agreement with the published crystal structure[22] and pattern 72–424 of the

DOI: 10.1039/b415435e

 This journal is © The Owner Societies 2005

powder diffraction file. No additional lines were detected. *trans*-$[Ru(NH_3)_4(H_2O)NO]Cl_3 \cdot H_2O$ was prepared as light orange needles from $[Ru(NH_3)_5NO]Cl_3 \cdot H_2O$ *via trans*-$[Ru(NH_3)_4(OH)NO]Cl_2$.[4] The product was obtained from a clear solution of *trans*-$[Ru(NH_3)_4(OH)NO]Cl_2$ in water and HCl (pH = 1) by slow evaporation of the solvent under vacuum at room temperature. The powder X-ray diffraction pattern fits the calculated pattern based on the published crystal structure[23] with respect to peak positions and intensities. No additional diffraction lines were detected.

The DSC (Mettler DSC 30) is equipped with two quartz windows inside and outside of the cryostat for light irradiation. The small needle like crystals, lying randomly distributed in an Al-crucible, were irradiated by the unpolarized light of a metal halide lamp (Osram HMI 575 W), narrowed by a set of broadband interference filters at 365 nm, 405 nm, 415 nm and 434 nm (FWHM = 10 nm) or by the monochromatic light of an Ar^+ laser (458 nm and 476.5 nm) with an intensity of $I =$ 180 mW cm^{-2}. The total exposure $Q = \int \mathrm{I} \mathrm{d}t$ on the sample to reach saturation amounts to about 2000 J cm^{-2}. The transfer from SI into SII was performed by subsequent irradiation with monochromatic light of a Nd-YAG laser ($\lambda = 1064$ nm) with an intensity of $I = 120$ mW cm^{-2} and a total exposure of $Q =$ 2250 J cm^{-2}. The dynamic measurements were performed at a linear heating rate $q = \mathrm{d}T/\mathrm{d}t = 4$ K min^{-1}. The corresponding spectrum of the unirradiated sample was subtracted, to give a horizontal baseline in the temperature range of the thermal decay. In this manner the heat release of the metastable states can be precisely determined. No phase transition was detected in the unirradiated sample between $T = 120$ K and $T = 330$ K. The detected signal of the DSC is the time derivative of the enthalpy $\mathrm{d}H/\mathrm{d}t$ in 10^{-3} Watt (mW) over the temperature. The total enthalpy is given by $H_{\mathrm{tot}} = \int (\mathrm{d}H/\mathrm{d}t)\mathrm{d}t$ and the activation energy E_A and frequency factor Z are obtained by fitting the curves to the equation

$$\frac{\mathrm{d}H(T)}{\mathrm{d}t} = H_{\mathrm{tot}} Z \exp\left(-\frac{E_A}{k_B T} - \frac{Z}{q}\int_{T_O}^{T} \exp\left(-\frac{E_A}{k_B T'}\right)\mathrm{d}T'\right) \tag{2.1}$$

which describes the dynamical DSC curve of an Arrhenius-like decay. k_B denotes the Boltzmann constant, q the heating rate, and T_0 is the starting temperature for the integration. Using the Arrhenius Ansatz for the reaction constant k

$$k(T) = Z \exp\left(-\frac{E_A}{k_B T}\right) \tag{2.2}$$

the fraction α of excited molecules decaying in time t is given by

$$\frac{\mathrm{d}\alpha}{\mathrm{d}t} = k(T) \times (1 - \alpha) \tag{2.3}$$

for first-order chemical reactions. Inserting $\mathrm{d}\alpha/\mathrm{d}t = q \times \mathrm{d}\alpha/\mathrm{d}T$ and integrating over T yields

$$1 - \alpha = \exp\left(-\frac{Z}{q}\int_{T_0}^{T} \exp\left(-\frac{E_A}{k_B T'}\right) dT'\right) \tag{2.4}$$

Inserting eqn. (2.4) in eqn. (2.3) and using $\frac{\mathrm{d}\alpha}{\mathrm{d}t} = \frac{1}{H_{\mathrm{tot}}}\frac{\mathrm{d}H}{\mathrm{d}t}$, one obtains eqn. (2.1). The integration in eqn. (2.1) is performed numerically over the corresponding temperature range yielding the three parameters H_{tot}, E_A and Z. The samples were irradiated at $T = 123$ K in an N_2 atmosphere. In order to demonstrate that the growth rate of the population as a function of the exposure Q is independent of the irradiation temperature we recorded two series $H_{\mathrm{tot}}(Q)$ at $T = 153$ K and $T = 243$ K. The temperature calibration with an accuracy of ± 1 K was performed using the phase transitions of In, Hg, pentane, $NH_4H_2PO_4$, and KH_2PO_4. The enthalpy was calibrated with the area of the In phase transition (28.45 J g^{-1}).

The DFT calculations were performed for the $[Ru(NH_3)_4(L)NO]^{2+,3+}$ ions (L = OH, NH_3, H_2O) using the PBE functional within the DMol^3 code[24,25] with the very accurate basis set DNP.[26] The local energy minima of the ground state energy surface (ground state GS, metastable state SI and metastable state SII) as well as the saddle points T0 connecting GS and SII and T1 connecting SII and SI were precisely determined.[27] The procedure to locate saddle points[27] does this without using a Hessian as input information. The necessary partial Hessians are calculated within that method, by numerical differentiation of energy gradients. This method is capable of locating saddle points as precisely as desired, with an efficiency coming close to the efficiency for finding minima. The saddle points have been confirmed by demonstrating vanishing of gradients and the existance of a single imaginary frequency. (This calculation uses a full Hessian from numerical differentiation of energy gradients). The energy surface is calculated along the 'quadratic synchronous transit' (QST),[28] part 1 is a QST passing exactly through GS-T0-SII and part 2 is a QST passing exactly through SII-T1-SI. The QST through the saddle points are approximations to the intrinsic reaction coordinate (IRC). Each of the present QST agrees with the IRC at the minima and the saddle point. In the rest of the text we will refer to this composite QST as the reaction coordinate Q. As the system moves along the reaction coordinate, the NO group rotates approximately about its bond-center, while the rest of the molecule stays with minor geometry changes. While it is N towards Ru at the GS, NO is *side-on* at SII (rotation of about 90°) and O towards Ru for SI (rotation of 180°).

III. Experimental results

Fig. 1 shows the thermal decay curves of the metastable states SI and SII in *trans*-$[Ru(NH_3)_4(H_2O)NO]Cl_3 \cdot H_2O$, plotted in the same figure. SI is directly obtained by irradiation with light of wavelength $\lambda = 405$ nm ($Q = 2000$ J cm^{-2}), while SII is populated in a two-step process: first irradiated with $\lambda = 405$ nm to obtain SI, which is subsequently transferred into SII with $\lambda = 1064$ nm. For a heating rate of $q = 4$ K min^{-1} the maxima of the heat release occur at 293(1) K and 223(1) K for SI and SII, respectively. The activation energies E_A and frequency factors Z are determined by fitting eqn. (2.1) to the curves of SI and SII. The results are: $E_A(\mathrm{SI}) = 0.95(3)$ eV, $E_A(\mathrm{SII}) = 0.69(3)$ eV, $Z(\mathrm{SI}) = 2 \times 10^{14}$ s^{-1}, $Z(\mathrm{SII}) = 3 \times 10^{13}$ s^{-1}. Note that the activation energy $E_A(\mathrm{SI}) = 0.95(3)$ eV is the

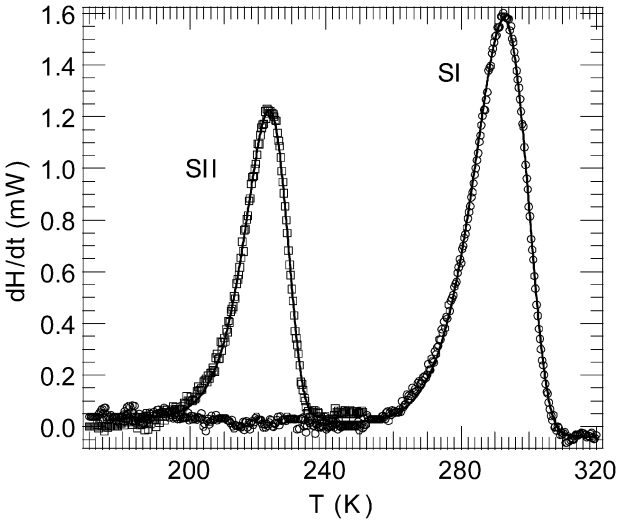

Fig. 1 Thermal decay curves ($q = 4$ K min^{-1}) of SI ($Q = 2000$ J cm^{-2}, $\lambda = 405$ nm) and SII ($Q_{405} = 2000$ J cm^{-2}, $\lambda = 405$ nm and $Q_{1064} =$ 2250 J cm^{-2}, $\lambda = 1064$ nm) in *trans*-$[Ru(NH_3)_4(H_2O)NO]Cl_3 \cdot H_2O$. Solid lines correspond to fits of eqn. (2.1). Fitted parameters: $E_A =$ 0.95(3) eV, $Z = 2 \times 10^{14}$ s^{-1} for SI and $E_A = 0.69(3)$ eV, $Z = 3 \times 10^{13}$ s^{-1} for SII. Irradiation was performed at $T = 153$ K.

highest ever found for such metastable states. The error in the determination of the frequency factors is about one order of magnitude due to the small temperature range of the measurement. For *trans*-$[Ru(NH_3)_4(OH)NO]Cl_2$ the observed activation energies and frequency factors are $E_A(SI) = 0.91(3)$ eV, $E_A(SII) = 0.60(3)$ eV, $Z(SI) = 6 \times 10^{14}$ s^{-1}, $Z(SII) = 1 \times 10^{13}$ s^{-1} as indicated in Table 1.

The population process of SI, as illustrated in Fig. 2a for irradiation with $\lambda = 434$ nm, can be described by the exponential function $H_{tot} = H_{inf,SI}\,[1 - \exp(-Q/Q_0)]$, and yields the saturation value of $H_{inf,SI} = 14.7(6)$ kJ mol^{-1} and the characteristic exposure $Q = 370(20)$ J cm^{-2}, which is a measure of the growth rate of the population. The transfer dynamics of SI $\rightarrow$ SII is presented in Fig. 2b. Here the starting configuration is always obtained by populating SI into saturation, using light of wavelength 434 nm and an exposure of 2000 J cm^{-2}. The transfer into SII is performed with a Nd-YAG laser ($\lambda =$ 1064 nm). The metastable state SI decreases exponentially as a function of the exposure Q according to $H_{tot} = H_{SI}\,[\exp(-Q/Q_{SI})]$ with $Q_{SI} = 1000(150)$ J cm^{-2} and SII increases according to $H_{tot} = H_{inf,SII}\,[1 - \exp(-Q/Q_{SII})]$ with $Q_{SII} = 820(100)$ J cm^{-2} and $H_{inf,SII} = 9.7(6)$ kJ mol^{-1}. About 30% of SI is transferred back into the ground state during this procedure.

The saturation value $H_{tot}(SI)$ of the population of SI shows a distinct wavelength dependence, as illustrated in Fig. 3. SI can only be populated when irradiating with light in the spectral range of 20 000–29 000 cm^{-1} (corresponding to 345–500 nm). The maximal population of $H_{tot} = 24.4(8)$ kJ mol^{-1} is obtained when irradiating with $\lambda = 405$ nm. For comparison we also measured the wavelength dependence of the population H_{tot} (SI) in the compound $[Ru(NH_3)_5NO]Cl_3 \cdot H_2O$, where the maximum is shifted to higher wavelengths (about 440 nm). This shift corresponds more or less to the shift of the ground state absorption band of the $Ru(d_{xy}) \rightarrow \pi$ (NO) transition from 426 nm in the former[23] to 447 nm in the latter.[29,30]

A further interesting and important result is that the population of SI depends on the irradiation temperature. In order to prove this, we have irradiated the sample at a temperature T_i. After ceasing irradiation the sample was cooled from T_i down to 130 K within 60 s, and then the thermal decay spectrum was recorded with a heating rate $q = 4$ K min^{-1}. As illustrated in Fig. 4a the population with light of wavelength 434 nm yields a saturation value of about 15 kJ mol^{-1} when illuminating at temperatures T_i below about 200 K. For illumination temperatures of 200–250 K the obtainable population decreases gradually to zero. Since the lifetime of SI at these temperatures is above 10^5 s, it is not possible that a measurable fraction of SI decays during the irradiation process, which takes about 10^4 s. The lifetimes of SI and SII, as calculated from the E_A and Z values, are indicated on the right axis. It can be seen that the decrease of the saturation population starts when the lifetime τ of SII drops below 10^3 s and vanishes completely when it drops below 10^{-1} s. The same experiment on the compound $[Ru(NH_3)_5NO]Cl_3 \cdot H_2O$ confirms these observations (see Fig. 4b). Here also, above $T = 200$ K, the population of SI decreases linearly with increasing temperature. For this compound the metastable state SI has its maximum in the heat flow at 260 K ($q = 4$ K min^{-1}), whereas SII lies at 223 K.[19] The data points in Fig. 4 are all obtained for an exposure of $Q = 2000$ J cm^{-2} and the wavelength $\lambda = 434$ nm. In order to check, whether the saturation population is obtained at all temperatures for $Q = 2000$ J cm^{-2}, we investigated the population process of SI at $T = 223$ K in *trans*-$[Ru(NH_3)_4(H_2O)NO]Cl_3 \cdot H_2O$. Fig. 5 shows the result. Indeed saturation is obtained at the same speed as for $T = 153$ K, as illustrated by the obtained parameters $Q_0 = 400(20)$ Ws cm^{-2} and $H_{inf,SI} =$ 8.8(3) kJ mol^{-1}. The implications of this temperature dependence are two-fold. First we have to note, although the lifetime of SI at 300 K is about 46 s, its generation is restricted to lower temperatures. Second it provides insight on the nature of the metastable states and their excitation pathway.

IV. Computational results

In order to elucidate this further we have performed ground state calculations for the PBE functional using the DMol^3 code[24,25] with the very accurate basis set DNP.[26] In addition to the well known local energy minima of the ground state energy

Table 1 Calculated potential surfaces of the ground state (GS) and the singlet excited state (ES) and energy barriers (eV). Observed activation energies E_A, frequency factors Z, and maximal enthalpy H_{max} determined *via* eqn. (2.1)

	E(GS)	E(T0)	E(T0) − E(SII)	E(SII)	E(T1)	E(T1) − E(SI)	E(SI)	Ref.
$[Ru(NH_3)_4(OH)NO]^{2+}$								This work
GS	0	2.24	0.66	1.58	2.88	1.17	1.71	
ES	2.54	2.55		3.29	3.23		3.24	
ES–GS	2.54	0.31		1.71	0.35		1.53	
E_A (exp.)/eV	0		0.60(3)			0.91(3)		
Z (exp.)/s^{-1}	0		1×10^{13}			6×10^{14}		
H_{max} (exp.)/kJ mol^{-1}	0		8.1(5)			14.4(5)		
$[Ru(NH_3)_5NO]^{3+}$								
GS	0	2.31	0.54	1.77	2.64	1.06	1.58	This work
E_A (exp.)/eV	0		0.66(3)			0.73(3)		19
Z (exp.)/s^{-1}	0		5×10^{12}			1×10^{12}		19
H_{max} (exp.)/kJ mol^{-1}	0		25.6(6)			39.2(6)		19
$[Ru(NH_3)_4(H_2O)NO]^{3+}$								This work
GS	0	2.43	0.72	1.71	Dissoc	Dissoc	1.63	
E_A (exp.)	0		0.69(3)			0.95(3)		
Z (exp.)/s^{-1}	0		3×10^{13}			2×10^{14}		
H_{max} (exp.)/kJ mol^{-1}	0		15.3(6)			24.3(6)		
$[Fe(CN)_5NO]^{2-}$								
GS	0	2.20	0.84	1.36	2.75	1.17	1.58	33
E_A (exp.)	0		0.52	0.95		0.67	1.05	31
Z (exp.)/s^{-1}	0		1×10^{15}			1×10^{13}		31
H_{max} (exp.)/kJ mol^{-1}	0		32.5			50.0		31

 This journal is © The Owner Societies 2005

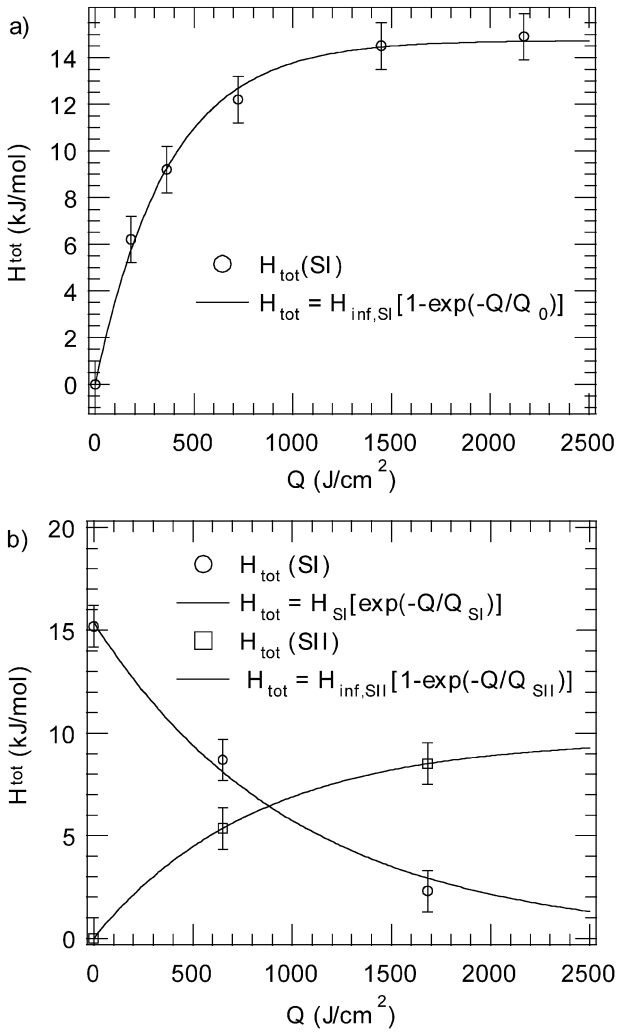

Fig. 2 (a) Increase of the integrated area of SI with increasing exposure Q in *trans*-$[Ru(NH_3)_4(H_2O)NO]Cl_3 \cdot H_2O$, when illuminating at $T = 153$ K. Fitted parameters: $H_{inf,SI} = 14.7(6)$ kJ mol^{-1}, $Q_0 = 370(20)$ J cm^{-2}. (b) Exponential decrease of the integrated area of SI and increase of SII with Q. Fitted parameters: $H_{SI} = 15.4(8)$ kJ mol^{-1}, $Q_{SI} = 1000(150)$ J cm^{-2}, $H_{inf,SII} = 9.7(6)$ kJ mol^{-1}, $Q_{SII} = 820(100)$ J cm^{-2}.

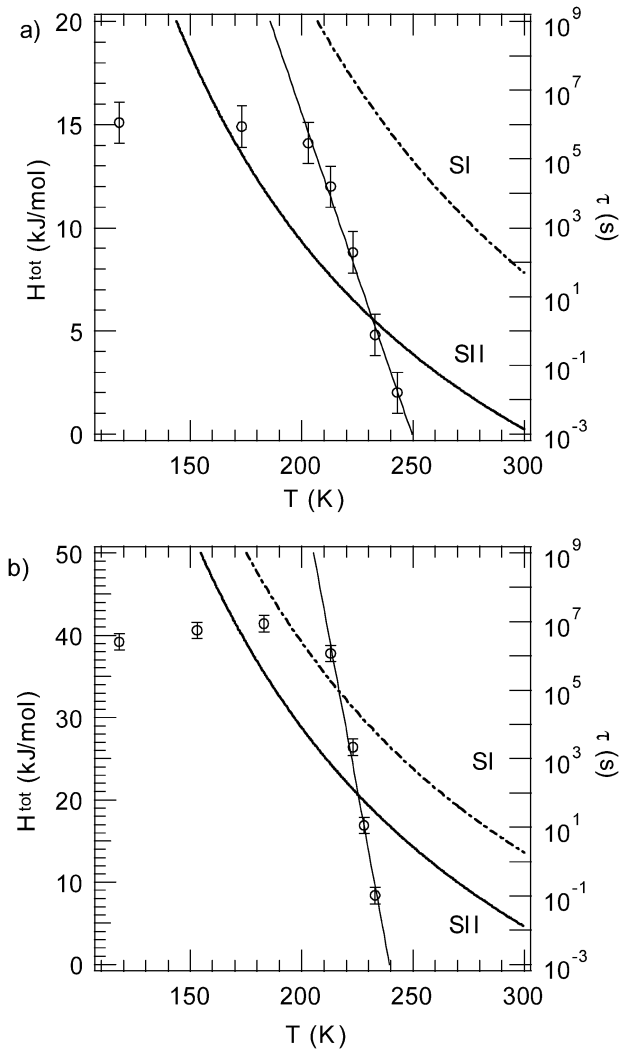

Fig. 4 Temperature dependence of the saturation population of SI in *trans*-$[Ru(NH_3)_4(H_2O)NO]Cl_3 \cdot H_2O$ (a) and $[Ru(NH_3)_5NO]Cl_3 \cdot H_2O$ (b). The solid lines correspond to fits using eqn. (5.5), yielding $b = 0.021(1)$ K^{-1} and $T_0 = 202(2)$ K (a) and $b = 0.037(3)$ K^{-1} and $T_0 = 212(2)$ K (b). The dashed and dash-dotted lines correspond to the lifetimes of SII and SI, respectively.

surface (ground state GS, metastable state SI and metastable state SII) we have precisely located the saddlepoints T0 connecting GS and SII and T1 connecting SII and SI. For geometrical reasons there is no saddle point directly connecting GS and SI, any connecting path passes through the SII basin. Fig. 6 shows a plot of the energy surface along the reaction

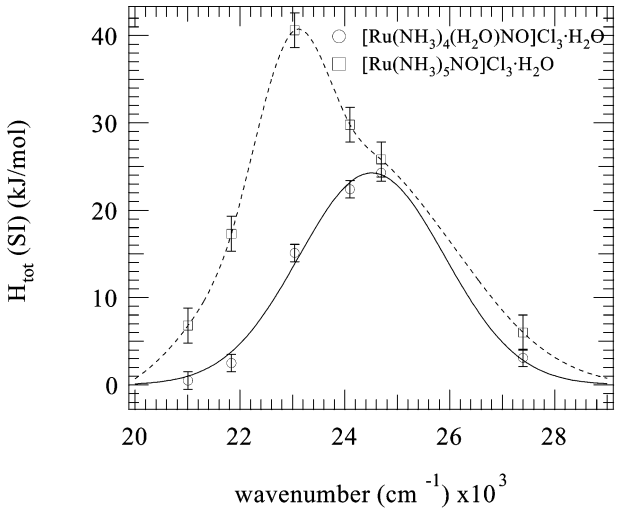

Fig. 3 Wavelength dependence of the saturation population of SI in *trans*-$[Ru(NH_3)_4(H_2O)NO]Cl_3 \cdot H_2O$ (○) and $[Ru(NH_3)_5NO]Cl_3 \cdot H_2O$ (□). The lines are guides to the eye.

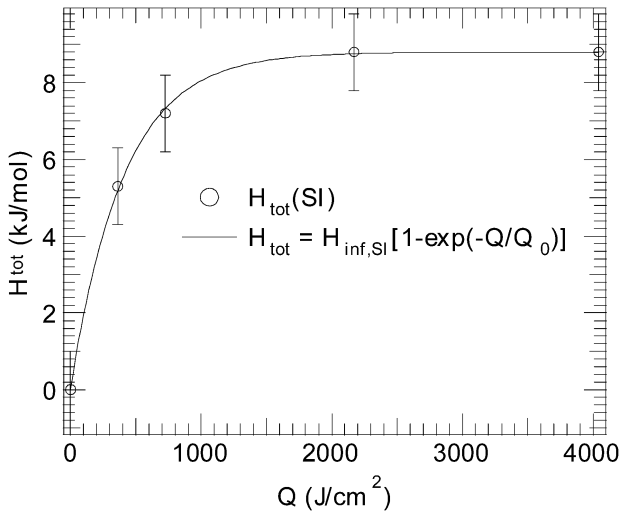

Fig. 5 Increase of the integrated area of SI with increasing exposure Q, when illuminating at $T = 223$ K in *trans*-$[Ru(NH_3)_4(H_2O)NO]Cl_3 \cdot H_2O$. Fitted parameters: $H_{inf,SI} = 8.8(3)$ kJ mol^{-1}, $Q_0 = 400(20)$ J cm^{-2}.

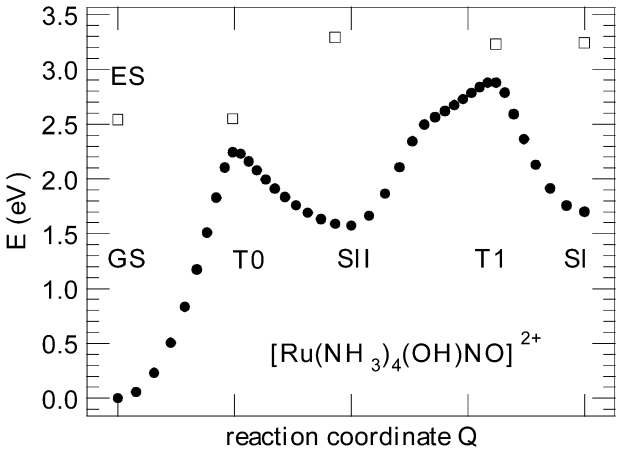

Fig. 6 Ground state potential surface (●) of *trans*-$[Ru(NH_3)_4(OH)NO]^{2+}$, illustrating the calculated energies of the minima GS ($E = 0$ eV), SII (1.58 eV), and SI (1.71 eV), as well as the saddle points T0 (2.24 eV) and T1 (2.88 eV). The reaction coordinate Q corresponds roughly to a rotation of the NO ligand by about 90° (SII) and 180° (SI). The empty squares indicate the calculated energetic positions for the first singlet excited state ES at the minima GS, SI and SII and the saddle points T0 and T1.

coordinate Q passing exactly through GS-T0-SII in the left half of the figure and continued right along the path SII-T1-SI. For a rough picture, this path corresponds to a rotation of the NO ligand by 180°. The SII structure is *side-on* bonded and forms a triangle RuNO, while SI corresponds to the *isonitrosyl* configuration RuON.

Table 1 summarizes the calculated energies of the potential surface for the molecules *trans*-$[Ru(NH_3)_4(OH)(NO)]^{2+}$, $[Ru(NH_3)_5NO]^{3+}$, *trans*-$[Ru(NH_3)_4(H_2O)NO]^{3+}$, and $[Fe(CN)_5NO]^{2-}$, as well as the observed activation energies E_A, frequency factors Z, and maximal obtainable enthalpies (populations) H_{max}. The energetic minima are denoted as GS, SI, and SII, while the saddle points are named T0 and T1 (compare also Fig. 6). The calculated energy differences $E(T0) - E(SII)$ and $E(T1) - E(SI)$ can be compared to the experimentally determined activation energies E_A. In order to visualize the possible optical excitation pathways, the energy values of the first singlet excited state potential surface (named ES) for the ion *trans*-$[Ru(NH_3)_4(OH)(NO)]^{2+}$ are calculated at the energetic minima GS, SI, and SII and the saddle points T0 and T1 of the ground state surface. From the difference $ES - E(GS)$ the small energetic differences between excited state and ground state potential surface at the saddle points are evident (see Table 1 and Fig. 6), which allow for the relaxation from the excited state surface into the metastable states SI and SII. As can be seen from Table 1 the saddle points T0 are all in the range $E(T0) = 2.20$–2.43 eV while the corresponding saddle points T1 are all lying in the higher energy range $E(T1) = 2.64$–2.88 eV. This agrees well with the experimental observation, that during the thermal decay of SII no occupation of SI was observed, indicating that the decay of SII occurs directly into GS. Furthermore in the ruthenium complexes with *trans* ligands H_2O and NH_3 the energetic position $E(SI)$ of SI is lower than that of SII ($E(SII)$), while for the compound with the *trans* ligand OH and the iron complex $[Fe(CN)_5NO]^{2-}$ the situation is reversed. The activation energies of SII are generally smaller than those of SI. From Table 1 it is clear that the calculated energy differences $E(T0) - E(SII)$ and $E(T1) - E(SII)$ overestimate the observed activation energies E_A for all cases except for $E(T0) - E(SII)$, which is equal to $E_A(SII)$, in $[Ru(NH_3)_5NO]^{3+}$, where the calculated value is 0.12 eV smaller than the observed 0.66 eV.

trans-$[Ru(NH_3)_4(H_2O)NO]Cl_3 \cdot H_2O$ has the highest known experimental activation energy (0.95 eV). In our calculations the saddle point T1 appears to fall above the dissociation limit of the free 3+ ion, and thus location of the saddle point was thwarted by dissociation. Fig. 6 therefore shows the results for the *trans*-$[Ru(NH_3)_4(OH)(NO)]^{2+}$ ion, which has an almost as high activation energy as *trans*-$[Ru(NH_3)_4(H_2O)NO]^{3+}$ ($E_A = 0.91$ eV, see Table 1).

For the complex $[Fe(CN)_5NO]^{2-}$ the energetic positions of the minima SI ($E(SI) = 1.05$ eV) and SII ($E(SII) = 0.95$ eV) are known from experiment.[31] Due to the fact that the activation energies and the ground state minima are overestimated by the calculation it is clear that also the saddle points are overestimated. However from a comparison of the values for SI and SII in the different compounds it is evident that the overestimation is not simply scaleable by a constant.

V. Discussion

The thermal decay of the light-induced metastable states SI and SII in *trans*-$[Ru(NH_3)_4(H_2O)NO]Cl_3 \cdot H_2O$ follows the Arrhenius law and is completely analogous to the decays found in the compounds investigated so far.[15–17] Notable are the high activation energies of 0.95 eV (SI) and 0.69 eV (SII) which, together with the frequency factors, are responsible for the long lifetimes at 300 K of $\tau_{SI} = 46$ s (SI), $\tau_{SII} = 0.013$ s (SII) for $[Ru(NH_3)_4(H_2O)NO]Cl_3 \cdot H_2O$. Comparing the lifetimes with $\tau_{SI} = 3.2$ s (SI), $\tau_{SII} = 0.0012$ s (SII) found in *trans*-$[Ru(NH_3)_4(OH)NO]Cl_2$ and $\tau_{SI} = 1.8$ s (SI), $\tau_{SII} = 0.0024$ s (SII) for the compound $[Ru(NH_3)_5NO]Cl_3 \cdot H_2O$,[19] where only the *trans*-ligand is changed from H_2O to OH and NH_3, one recognizes that a sufficiently long lifetime for applications may be possible by choosing the appropriate *trans*-ligand in such complexes. Likewise the exponential population dynamics of SI and the transfer behavior of SI → SII, as illustrated in Fig. 2, are completely analogous to other complexes exhibiting metastable states. However, we have to bear in mind, that the population of SI depends on the irradiation temperature, as shown in Fig. 4. The striking feature of this temperature dependence of the population $H_{tot}(T)$ is the onset of a linear decrease of the population with increasing temperature around 200 K. Note that this is no phase transition with long range cooperative behavior, since the isothermal decays of the metastable states are mono-exponential and SI is also stable in cooled solutions.[15] The metastable states are local molecular states. The released enthalpy is given by the product of the number of decaying molecules n_Q in the metastable state and the energetic position E of the metastable state with respect to the ground state: $H = P \times E \times 96.490$, when H is given in kJ mol^{-1}, E in eV, and the population is given by $P = n_Q/n_0$, n_0 being the total number of molecules. Since E is constant, *e.g.*, 1.05 eV (SI) and 0.95 eV (SII) in SNP, the temperature dependence is determined by the population P (T): $H(T) = P(T) \times E \times 96.490$. Normalizing to the maximal obtainable population H_{max} we obtain $H(T)/H_{max} = P(T)/P_{max}$. Due to the linear dependence $H(T)$ above a starting temperature T_0 we obtain: $H(T) = H_{max} + a(T_0 - T)$ for $T \geq T_0$ and therefore

$$\frac{H(T)}{H_{max}} = \frac{P(T)}{P_{max}} = 1 + \frac{a}{H_{max}}(T_0 - T) = 1 + b(T_0 - T). \quad (5.5)$$

The values $b = 0.021(1)$ K^{-1} and $T_0 = 202(2)$ K (H_2O) and $b = 0.037(3)$ K^{-1} and $T_0 = 212(2)$ K (NH_3) are obtained from the fit, as illustrated in Fig. 4. This linear dependence is notably different from the temperature dependence of the population of SI found in SNP,[31] which exhibits a population curve with two plateaus and below about 130 K the maximum population of 50 kJ mol^{-1} is obtained. Using the calculated values $E(SI)$ and $E(SII)$ we can estimate the population P from the observed enthalpy H_{max}, obtaining 15% for SI and 9% for SII in *trans*-$[Ru(NH_3)_4(H_2O)NO]Cl_3 \cdot H_2O$. Considering that the calculated energies $E(SI)$ and $E(SII)$ are most probably

This journal is © The Owner Societies 2005

overestimated, these values represent lower bounds for the obtainable maximal population. In the same manner we obtain the values 8.7% for SI and 5.3% for SII for *trans*-[Ru(NH$_3$)$_4$(OH)NO]Cl$_2$, as well as for [Ru(NH$_3$)$_5$NO]Cl$_3$ · H$_2$O: 26% for SI and 15% for SII.

Comparing experimental and theorectical data in Table 1, it is clear that the calculation estimates a few tenths eV too high energies for the ground state energy surface. If that is corrected one recognizes that the T1 barrier is not higher than the ES above the GS energy. Incidentally, the qualitative picture is as shown in Fig. 1 in ref. 33, where more approximate methods were used to guess the barrier heights. Furthermore we note that the calculated activation energies E(T1) − E(SI), though ≈0.3 eV too high compared with the observed values, reflect the increasing values achieved by exchanging the *trans*-ligand NH$_3$ in [Ru(NH$_3$)$_5$NO]Cl$_3$ · H$_2$O by OH in *trans*-[Ru(NH$_3$)$_4$(OH)NO]Cl$_2$, and by H$_2$O *trans*-[Ru(NH$_3$)$_4$(H$_2$O)NO]Cl$_3$ · H$_2$O. The fact that the calculated saddle point T1 in *trans*-[Ru(NH$_3$)$_4$(H$_2$O)NO]Cl$_3$ · H$_2$O falls above the dissociation limit indicates also that the achievable activation energies and therefore also the lifetimes of the metastable states are limited by the dissociation barrier and that we are already near to this limit in these ruthenium complexes.

The picture sketched in Fig. 6 admits a single photon population process for SI, as well as the two-step process GS → SII → SI, which was already suggested in ref. 33 and taken up in ref. 32. In the single step process the molecule can relax directly into the SI basin after vertical excitation with blue light to the excited state energy surface, *i.e.* there is enough energy for the rotation of the NO ligand by 180°. If the excess energy over the barrier gets too high (shorter wavelengths) the trapping efficiency in the SI basin goes down, as the NO may rotate further and drop back into the GS configuration. The onset of the excitation may be not entirely sharp due to phonon absorption processes. This process is in qualitative agreement with Fig. 3. The onset of population near 21 000 cm^{-1} is consistent with a T1 value of 2.6 eV for *trans*-[Ru(NH$_3$)$_4$(H$_2$O)NO]Cl$_3$ · H$_2$O.

For the two-step process a first excitation and relaxation into the SII basin occurs (rotation of NO by about 90°), from where in a second excitation–relaxation step the SI basin is reached (another rotation by about 90°), or the molecules fall back into the GS. However, we have to stress here, that the experimental results show that no measurable fraction of the molecules remains in the SII basin during the population process. Therefore we can adhere as a necessary boundary condition for this two-step process that the absorption in the blue spectral range is much stronger for SII than for GS. Otherwise we would expect some molecules to be captured in the SII configuration during the population process of SI.

As already suggested in ref. 19, the obtainable saturation population indicates that during the irradiation a steady-state situation is setup, where an equilibrium between population into the state SI and depopulation out of SI is established. The observed dependence of the saturation population (Fig. 4) on the irradiation temperature T_i shows that this equilibrium is changed as a function of T_i. In a kinetic model of the population process this may be explained with a temperature dependence of the corresponding population or depopulation cross sections involved in the process. Hypothetically the observed temperature dependence of the population of SI might also be explained by the temperature dependence of the potential surface of the singlet excited state ES, through which the optical population and depletion of the metastable state SI occurs.

The presented thermodynamic measurements can be well explained by the geometrical model for the metastable states, calculated by DFT. This is in contrast to earlier neutron diffraction measurements on SI,[21] but in agreement with an earlier X-ray study.[20] While the *side-on* structure of the metastable state SII is evident from Fourier difference maps[20] the analysis of the *isonitrosyl* structure of SI is more involved, as the positions of NO and ON are overlapping and a considerable fraction of the molecules remains in the ground state. In all structural investigations of SI[20,21,34–36] the decision whether SI is formed by the *isonitrosyl* (ON) or the nitrosyl (NO) configuration is based on the discussion of the thermal displacement parameters of N and O. Furthermore the long lifetime of the metastable states cannot be explained by small structural changes, as already pointed out earlier[37] and discussed also in ref. 21. The presented thermodynamic measurements do not suffer from the above mentioned problems, as they allow the determination of the activation energies and energetic positions of the metastable states independently of the amount of population. Furthermore the wavelength- and temperature-dependent results can be described satisfactorily within the geometrical model provided by the DFT calculations. This model describes also adequately both metastable states in a series of compounds by reflecting well the observed increase of the activation energy as a function of ligand-exchange, which cannot be explained by the small structural changes as reported in ref. 21.

VI. Conclusions

In summary, we have presented experimental and theoretical evidence for the metastable states SI and SII in *trans*-[Ru(NH$_3$)$_4$(H$_2$O)NO]Cl$_3$ · H$_2$O and *trans*-[Ru(NH$_3$)$_4$(OH)NO]Cl$_2$ and have described their population and transfer behavior. The lifetimes of the metastable states can be tuned by choosing the appropriate ligands, *e.g.*, $\tau_{SI} = 46$ s and $\tau_{SII} = 0.013$ s at 300 K for *trans*-[Ru(NH$_3$)$_4$(H$_2$O)NO]Cl$_3$ · H$_2$O, while $\tau_{SI} = 3.2$ s and $\tau_{SII} = 0.0012$ s for *trans*-[Ru(NH$_3$)$_4$(OH)NO]Cl$_2$. It was shown that the population of SI depends on the irradiation temperature, and is only possible at low enough temperatures, when using a continuous-wave source for irradiation. The wavelength dependence of the population of SI was described experimentally and could be explained within a potential picture calculated by DFT, based on the assumption that the NO ligand undergoes a rotation induced by light irradiation. The calculated energies of saddle points and minima in the ground state potential surface are in good agreement with the measured activation energies. The population and depopulation processes can be satisfactorily described within this picture.

Acknowledgements

Financial support by the Swiss National Science Foundation (PBEZ2-100873), the Deutsche Forschungsgemeinschaft (WO618/5-1) and INTAS (No. 2000-0651) is gratefully acknowledged.

References

1 M. J. Clarke, *Coord. Chem. Rev.*, 2003, **236**, 209.
2 P. G. Wang, M. Xian, X. P. Tang, X. J. Wu, Z. Wen, T. W. Cai and A. J. Janczuk, *Chem. Rev.*, 2002, **102**, 1091.
3 A. Joly and C. R. Hebd, *Acad. Sci.*, 1890, **111**, 969.
4 K. Gleu and I. Büddecker, *Z. Anorg. Allg. Chem.*, 1952, **268**, 202.
5 A. F. Schreiner, S. W. Lin, P. J. Hauser, E. A. Hopcus, D. J. Hamm and J. D. Gunther, *Inorg. Chem.*, 1977, **11**, 880.
6 S. Pell and J. N. Armor, *Inorg. Chem.*, 1973, **12**, 873.
7 D. Guenzburger, A. Garnier and J. Danon, *Inorg. Chim. Acta*, 1977, **21**, 119.
8 N. M. Sinitsyn, G. G. Novitskii, I. A. Khartonik, V. V. Borisov and A. B. Kovrikov, *Russ. J. Inorg. Chem.*, 1982, **27**, 1152.
9 O. V. Sizova, O. O. Lyubimova and V. V. Sizov, *Russ. J. Gen. Chem.*, 2004, **74**, 317.
10 E. Tfouni, M. Krieger, B. R. McGarvey and D. W. Franco, *Coord. Chem. Rev.*, 2003, **236**, 57.
11 R. M. Carlos, A. A. Ferro, H. A. S. Silva, M. G. Gomes, S. S. S. Borges, P. C. Ford, E. Tfouni and D. W. Franco, *Inorg. Chim. Acta*, 2004, **357**, 1381.

12 M. Imlau, T. Woike, R. Schieder and R. A. Rupp, *Phys. Rev. Lett*., 1999, **82**, 2860.
13 M. Imlau, S. Haussühl, T. Woike, R. Schieder, V. Angelov, R. A. Rupp and K. Schwarz, *Appl. Phys. B*, 1999, **68**, 877.
14 U. Hauser, V. Oestreich and H. D. Rohrweck, *Z. Phys. A*, 1977, **280**, 17.
15 H. Zöllner, W. Krasser, Th. Woike and S. Haussühl, *Chem. Phys. Lett*., 1989, **161**, 497.
16 K. Ookubo, Y. Morioka, H. Tomizawa and E. Miki, *J. Mol. Struct*., 1996, **379**, 241.
17 P. Coppens, I. Novozhilova and A. Kovalevski, *Chem. Rev*., 2002, **102**, 861.
18 H. Zöllner, W. Krasser, Th. Woike and S. Haussühl, *Z. Kristallogr*., 1989, **188**, 139.
19 D. Schaniel, T. Woike, C. Boskovic and H. U. Güdel, *Chem. Phys. Lett*., 2004, **390**, 347.
20 M. D. Carducci, M. R. Pressprich and P. Coppens, *J. Am. Chem. Soc*., 1997, **119**, 2669.
21 D. Schaniel, J. Schefer, M. Imlau and T. Woike, *Phys. Rev. B*, 2003, **68**, 104108.
22 F. Bottomley, *J. Chem. Soc., Dalton Trans*., 1974, **15**, 1600.
23 C. W. B. Bezerra, S. C. da Silva, M. T. P. Gambardella, R. H. A. Santos, L. M. A. Plicas, E. Tfouni and D. W. Franco, *Inorg. Chem*., 1999, **38**(25), 5660.
24 B. Delley, *J. Chem. Phys*., 1990, **92**, 508.
25 B. Delley, *Phys. Rev. B*, 2002, **66**, 155125.
26 B. Delley, *J. Chem. Phys*., 2000, **113**, 7756.
27 N. Govind, M. Petersen, G. Fitzgerald, D. King-Smith and J. Andzelm, *Comput. Mater. Sci*., 2003, **28**, 250.
28 Th. A. Halgren and W. N. Lipscomb, *Chem. Phys. Lett*., 1977, **49**, 225.
29 S. C. DaSilva and D. W. Franco, *Spectrochim. Acta, Part A*, 1999, **55**, 1515.
30 S. I. Gorelsky, S. C. DaSilva, A. B. P. Lever and D. W. Franco, *Inorg. Chim. Acta*, 2000, **300–302**, 698.
31 T. Woike, W. Krasser, H. Zöllner, W. Kirchner and S. Haussühl, *Z. Phys. D*, 1993, **25**, 351.
32 S. I. Gorelsky and A. B. P. Lever, *Int. J. Quantum Chem*., 2000, **80**, 636.
33 B. Delley, J. Schefer and Th. Woike, *J. Chem. Phys*., 1997, **107**, 10067.
34 D. Fomitchev and P. Coppens, *Inorg. Chem*., 1996, **35**, 7021.
35 M. Kawano, A. Ishikawa, Y. Morioka, H. Tomizawa, E. Miki and Y. Ohashi, *J. Chem. Soc., Dalton Trans*., 200014), 2425.
36 A. Puig-Mollina, H. Müller, A.-M. Le Quéré, G. Vaughan, H. Graafsma and A. Kvick, *Z. Anorg. Allg. Chem*., 2000, **626**, 2379.
37 H. U. Güdel, *Chem. Phys. Lett*., 1990, **175**, 262.

 This journal is © The Owner Societies 2005